Journal of Alloys and Compounds 311 (2000) 288–291
Journal of ALLOYS AND COMPOUNDS
www.elsevier.com/locate/jallcom

Micro-crystalline C14 Laves phase in melt-spun AB_2 type Zr-based alloy

K.Y. Shu[a,b,*], Y.Q. Lei[a], X.G. Yang[a], S.K. Zhang[a], G.L. Lü[c], H. Zhang[b], Q.D. Wang[a]

[a]*Department of Materials Science and Engineering, Zhejiang University, Hangzhou 310027, PR China*
[b]*Shanghai Institute of Metallurgy, Chinese Academy of Sciences, Shanghai 200050, PR China*
[c]*Center Laboratory, Zhejiang University, Hangzhou 310028, PR China*

Received 18 April 2000; accepted 21 June 2000

Abstract

The single phase of micro-crystalline C14 Laves of $Zr_{0.7}Ti_{0.3}(NiVMnCr)_{2.1}$ alloy was successfully prepared by melt-spinning processing with a certain cooling rate. The investigation with XRD Rietveld analysis and TEM showed that micro-crystalline C14 Laves phase had a unique microstructure, the grain was composed of staked *c*-axis textured thin plates which contained a lot of crystallites with the mean size of about $3.1\times3.1\times1$ nm^3. The electrochemical measurement showed that it had longer cycle life, more activation cycles and lower discharge capacity than those of conventional mixture C14+C15 Laves phase. © 2000 Elsevier Science S.A. All rights reserved.

Keywords: Hydrogen storage alloy; Melt-spinning; Micro-crystalline C14 Laves phase; XRD Rietveld analysis

1. Introduction

Laves phase AB_2 alloys have attracted great attention as negative electrodes of rechargeable Ni/MH batteries because of their large capacity [1–4] and better resistance to oxidation than those of AB_5 alloys [5,6]. Many studies such as multiple alloying [3–5], chemical treating [7,8] and other methods [9,10] have been conducted on these alloy electrodes for improving their electrochemical performance. Although many reports revealed that the durability of AB_5 alloys was greatly improved by melt-spinning or atomization processing, there were only sporadic reports concerned with melt-spun or atomized AB_2 alloys. Ciureanu et al. found the melt-spun $ZrNi_2$ alloy was completely amorphous [11]. Fujiwara et al. studied several AB_2 type alloys and also found that C14 Laves phase in those melt-spun alloys were amorphous with trace crystalline [12]. Our former research showed that the melt-spun $Zr(NiMnCr)_{2.1}$ alloy were composed of crystalline C14 and C15 phase and C14/C15 phase weight ratio increased with the cooling rate [13]. Interestingly, that crystalline C14 Laves phase in melt-spun $Zr(NiMnM)_{2.1}$ alloy had a distinct micro-crystalline structure, which was quite different from the conventional as-cast C14 Laves phase alloy. Meanwhile, the hydrogen-storage capacity and durability were greatly improved in the melt-spun alloy which contains a small amount of micro-crystalline C14 Laves phase [14]. For identifying clearly the microstructure and the electrochemical properties for the C14 Laves phase of AB_2 Zr-based alloy prepared by melt-spinning, it is necessary to obtain single C14 Laves phase material. In this paper, we report that the $Zr_{0.7}Ti_{0.3}(NiVMnCr)_{2.1}$ alloy with single C14 phase is obtained by controlling cooling rate using melt-spinning technique and its electrochemical behaviors, which is different from those of conventional C14 Laves phases in as-cast alloy.

2. Experimental details

2.1. Sample preparation

The as-cast alloys of $Zr_{0.7}Ti_{0.3}(NiVMnCr)_{2.1}$ were prepared by arc melting under argon atmosphere with remelting 4 times to ensure homogeneity, and solidified in water-cooled copper crucible. Ribbons of melt-spun alloy were produced in a melt-spinning machine. The high cooling rate of about 4.3×10^5 K s^{-1} was controlled to ensure the alloy to form single micro-crystalline (MC) C14 Laves phase. The estimation of the cooling rate was reported in references [13,15]. The purity of the constituent metals was all above 99.95%. The melt-spun and as-cast

*Corresponding author. Fax: +86-21-6225-4273.
E-mail address: sky@itsvr.sim.ac.cn (K.Y. Shu).

0925-8388/00/$ – see front matter © 2000 Elsevier Science S.A. All rights reserved.
PII: S0925-8388(00)01084-7

alloys were mechanically grounded into powders below 300 mesh for electrode preparation and XRD experiment.

2.2. XRD and TEM analyses

Powder X-ray diffraction (XRD) measurement was conducted in a Rigaku D/max-IIIB diffractometer with a Cu Kα radiation. The diffraction patterns were analyzed by Rietveld method using LS1 software [16] for refinement of crystal structure and calculation of phase abundance. More detail information about the XRD experiment was introduced in Ref. [17]. The microstructure was observed and analyzed by transmission electron microscope (TEM). The thin foil sample for TEM testing was prepared by ion sputtering thinning method.

2.3. Electrochemical analysis

About 100 mg alloy powder were uniformly mixed with fine copper powder (−300 mesh) in the weight ratio of 1:2 and then pressed into pellets as electrodes. Electrochemical properties were tested in a standard trielectrode test cell open to the atmosphere. A $Ni(OH)_2$/NiOOH electrode was used as the counter electrode and Hg/HgO/OH^- used as the reference electrode. The electrolyte was a 6 M KOH solution. The electrodes were fully charged at 100 mA g^{-1} and discharged at 50 mA g^{-1}. The discharge cut-off potential was set at −0.6 V with respect to the Hg/HgO/OH^- reference electrode. The testing temperature was 25°C.

3. Results and discussion

3.1. XRD and TEM analysis

Fig. 1 shows a typical XRD pattern of an alloy of $Zr_{0.7}Ti_{0.3}(NiVMnCr)_{2.1}$ melt-spun at cooling rate of about 4.3×10^5 K s^{-1}. Obviously, it is not amorphous and all diffraction peaks can be reasonably attributed to the C14 Laves phase. As known, the microstructure of the melt-spun alloy is mainly dependent upon the composition, melt temperature and cooling rate. In melt-spun $Zr(NiVMnCr)_{2.1}$ was composed of micro-crystalline (MC) C14 and C15, and the weight ratio of C14 to C15 Laves phase is dependent upon cooling rate [13]. Obviously here single C14 phase has been obtained at the given cooling rate for $Zr_{0.7}Ti_{0.3}(NiVMnCr)_{2.1}$ alloy. The detail analysis of XRD data with Rietveld method for a $Zr_{0.7}Ti_{0.3}(NiVMnCr)_{2.1}$ alloy is summarized in Table 1. The fit of goodness of the Rietveld analysis is 2.59, which shows the analysis is in the scope of the accuracy of the method. For comparison, the XRD data of the C14 Laves phase in as-cast alloy with the same composition are also list in Table 1. It is clear that, compared with conventional

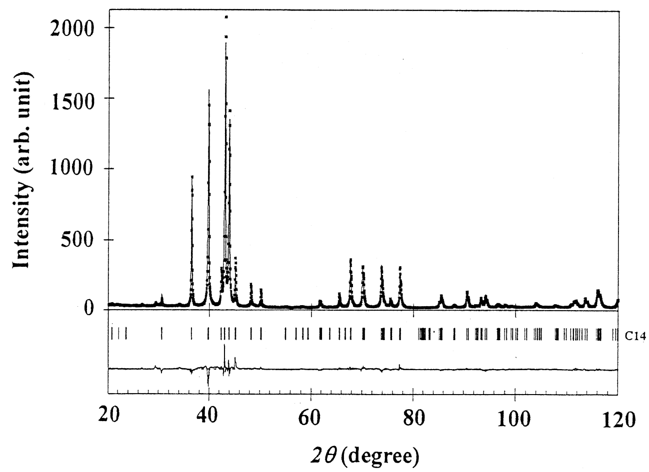

Fig. 1. Observed (· · ·), calculated (———) and difference (bottom, ———) XRD pattern of micro-crystalline C14 Laves phase in melt-spun $Zr_{0.7}Ti_{0.3}(NiVMnCr)_{2.1}$ alloy.

C14 Laves phase in as-cast alloy, the cell parameters and volume of the MC C14 Laves phase in melt-spun alloy are contracted, for example, about −1.74% in volume. Rietveld analysis also indicates that the crystallite size in melt-spun C14 phase is much smaller than that in as-cast C14 phase. It is about 3.1×3.1×1 nm for MC C14 phase and about 18.3×18.3×7.4 nm for the conventional C14 phase. Table 1 also gives the micro-strain in cells of both MC and conventional C14 Laves phase. The micro-strain is about 1×10^{-5} in *a*- and *c*-axis direction of conventional C14 Laves phase, indicating the uniform strain distribution. But the micro-strain in *c*-direction of MC C14 Laves phase is 1×10^{-3}, which is 2 orders of magnitude larger than 1×10^{-5} in the *a*-axis direction, and also that in both *a*- and *c*-axis of the as-cast C14 Laves phase. The above results indicate that there are strong anisotropic stresses and strains in the MC C14 Laves phase. We believe that the anisotropic behavior would affect the properties of the MC C14 Laves phase.

Fig. 2 is a typical microstructure picture of the MC C14 Laves phase under transmission electron microscopy (TEM). It indicates that the grain size with large angle boundary in melt-spun C14 Laves phase is around a micrometer and is composed of very thin plates, which are stacked parallell to each other as a lamellar structure. Or say all plates are textured along the *c*-axis for stacking. According to XRD Rietveld analysis, each thin plate contains many minute crystallites with a size of about 3.1×3.1×1 nm^3. For convenience, we call this C14 phase with such a microstructure the micro-crystalline (MC) C14 Laves phase in this text. Such a unique microstructure of C14 Laves phase was firstly observed in melt-spun alloy $Zr(NiVMnCr)_{2.1}$ [13], but there MC C14 Laves phase coexists with C15 Laves phase. As pointed out, the appearance of MC C14 is closely connected with rapid cooling rate from the melt [13]. This lamellar structure of

Table 1
XRD results of the alloy $Zr_{0.7}Ti_{0.3}(NiVMnCr)_{2.1}$ prepared by melt-spinning and as-cast methods

Solidification methods	Cell parameters			Crystallite size		Micro-strain in cell	
	a (nm)	*c* (nm)	*V* (nm^3)	M_{11} (nm)	M_{33} (nm)	$\langle \epsilon_{11}^2 \rangle^{1/2}$	$\langle \epsilon_{33}^2 \rangle^{1/2}$
Melt-spinning	0.4936	0.8041	0.1697	3.1	1.0	1×10^{-5}	1×10^{-3}
As-cast	0.4964	0.8093	0.1727	18.3	7.4	1×10^{-5}	1×10^{-5}

stacked plates in the grain is quite different from conventional C14 Laves phase in as-cast alloy shown in Ref. [18]. To our knowledge, this is the first observation of a single C14 Laves phase with micro-crystalline microstructure obtained by melt-spinning. For a given alloy composition, the cooling rate is a controlling factor for microstructure and phase composition. From the above results, it is believed that the high cooling rate of above 4.3×10^5 K s^{-1} is enough to suppress the nucleation and growth of C15 Laves phase in $Zr_{0.7}Ti_{0.3}(NiVMnCr)_{2.1}$. It is necesary to further study why the cooling rate can affect the weight ratio of C14 phase to C15 phase. Also, it seems that the anisotropy of the growing rate in the *a–b* plane and *c*-axis direction plays an important role for plate lamellar microstructure under rapidly solidified conditions, i.e., fast cooling rate causes more C14 nucleation and increases the ratio of growing rate in the *a–b* plane to the *c*-axis direction of C14 Laves phase.

3.2. Electrochemical properties

The effect of MC C14 Laves phase on the hydrogen storage capacity of melt spun (C14+C15) composite of $Zr(NiVMnCr)_{2.1}$was reported before [14]. Here more detail concerned with electrochemical properties, such as activation process, discharge capacity and cycle stability, for pure MC C14 Laves phase in melt-spun $Zr_{0.7}Ti_{0.3}(NiVMnCr)_{2.1}$ are given. Fig. 3 shows activation process of both MC C14 Laves phase in melt-spun alloy and mixed conventional (C14+C15) Laves phases in as-cast alloy. For pure MC C14, the curve presents an 'S' shape. In first three cycles, the discharge capacity rises slowly and then goes up quickly. After eight cycles the discharge capacity increases slowly again and reaches a maximum discharge capacity of 220 mAh g^{-1} at the 23rd cycle. The activation of melt-spun alloy with pure MC C14 Laves phase is difficult compared to that of as-cast alloy with C14 and C15 phase composite, which is completely activated within 10 charging–discharging cycles. Meanwhile, the discharge capacity of pure MC C14 phase alloy is much lower than that of as-cast alloy with the mixture of C14 and C15 Laves phase, as later the maximum discharge capacity reaches 350 mAh g^{-1}. The cycle stability of both alloys is shown in Fig. 4. The discharge capacity of MC C14 Laves phase decays very slowly. After 700 cycles its discharge capacity still remains 190 mAh g^{-1}, and the average capacity decay rate ($\Delta C/\Delta N$) is about 0.0429 mAh g^{-1} per cycle, which is much smaller than the value of 0.2357 mAh g^{-1} per cycle for as-cast alloy. One could argue that the smaller capacity decay rate is a result of the

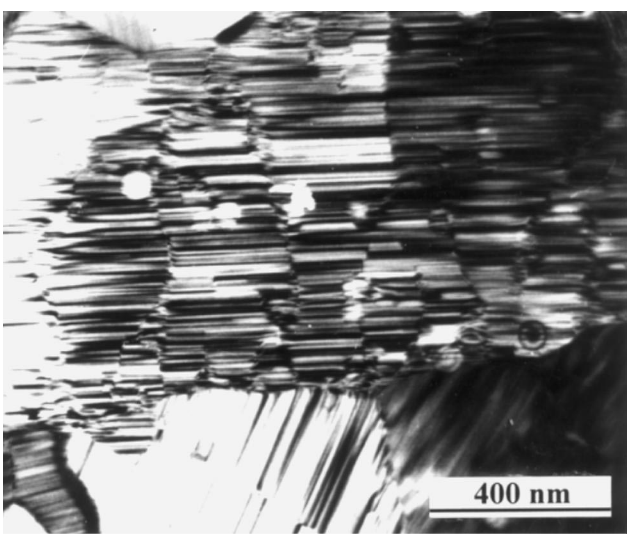

Fig. 2. Microstructure of micro-crystalline C14 Laves phase in melt-spun $Zr_{0.7}Ti_{0.3}(NiVMnCr)_{2.1}$ alloy.

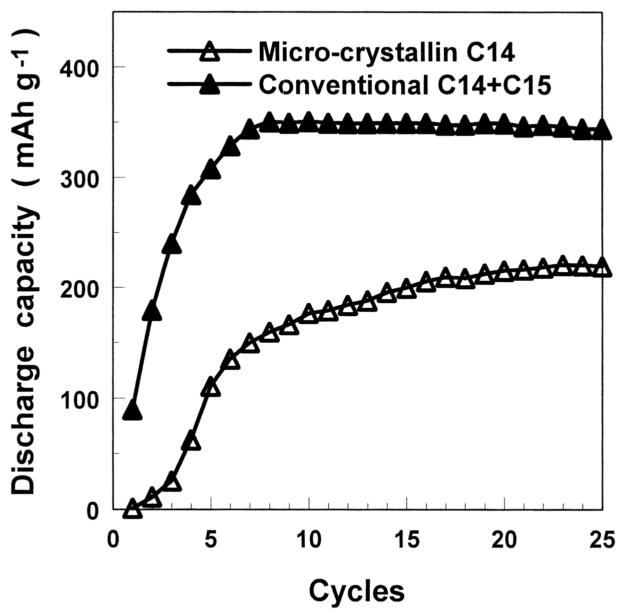

Fig. 3. Activation process of the electrodes made from melt-spun and as-cast $Zr_{0.7}Ti_{0.3}(NiVMnCr)_{2.1}$ alloys.

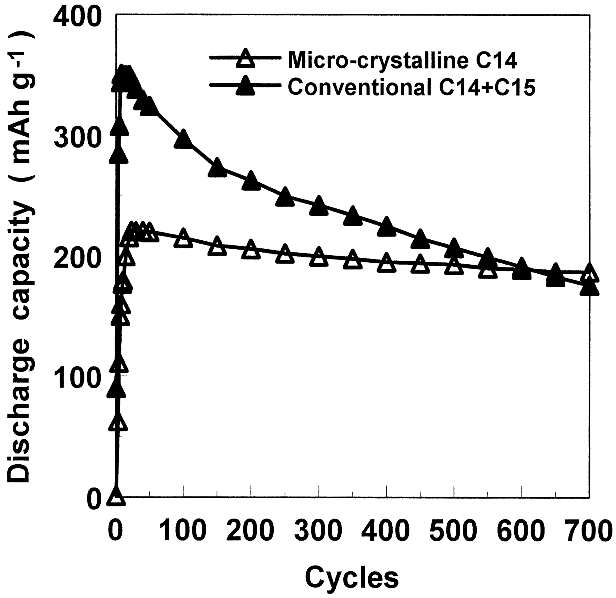

Fig. 4. Cycle life of the electrode made from melt-spun and as-cast $Zr_{0.7}Ti_{0.3}(NiVMnCr)_{2.1}$ alloys.

smaller storage capacity and thus less pronounced lattice expansion. However, even the capacity decreases to 190 mAh g^{-1} after 600 cycles; the capacity decrease rate of MC C14 alloy is smaller. The unique microstructure, contracted cell volume and anisotropic stress field in the cell of the MC C14 Laves phase should be responsible for the change of electrochemical properties.

Because of its fine grain and lamellar structure of thin plates, there are lots of interfaces in the MC C14 Laves phase, which may cause a decrease of the effective volume of storing hydrogen. Meanwhile, the large anisotropic stress and strain in the cell of the MC C14 phase would imply that some of the tetrahedral interstitial may be so strained as to be ineffective as a hydrogen storage position. In addition, the decrease of cell parameters and volume in the MC C14 phase would cause the contraction of the interstitial space and thus the effect of strain on the number of effective hydrogen storage position becomes obvious. The above factors combined together cause a great decrease of discharge capacity of melt-spun alloy with pure MC C14 Laves phase. The anisotropy stress field causes the alloy require more activation cycles through lowering the hydrogen diffusion rate. The long cycle life of the alloy with the MC C14 Laves phase could be also understood from its special microstructure. It is well accepted that the cycle life is closely connected with the pulverization rate of hydride powders owing to the volume expansion in the hydrogen-absorbing process. The interface can partly relax the stress from the volume expansion. Lots of interfaces, including grain boundaries and interfaces between thin plates, in the MC C14 phase would provide local stress relaxation to delay pulverizing of the MC 14 phase powder.

4. Conclusion

Pure micro-crystalline C14 Laves phase has been successfully produced by melt-spinning with a high cooling rate for $Zr_{0.7}Ti_{0.3}(NiVMnCr)_{2.1}$. The XRD and TEM investigation shows that it has a unique microstructure. The fine grain of MC C14 phase is composed of many thin plate subgrains, which are stacked parallell to each other with a *c*-axis texture. Each plate contains a lot of crystallites with a size of about $3.1\times3.1\times1$ nm^3. The stress and strain in the cells of the MC C14 Laves phase show strong anisotropy. Because the lamellar structure of MC C14 Laves phase is full of interfaces and benefits the resistance to pulverization in absorbing hydrogen, the alloy with the MC C14 Laves phase has a longer cycle life. Anisotropy of strain and stress fields could lower the hydrogen diffusion and make the MC C14 Laves phase need more activation cycles. The contract cell volume and anisotropy of strain and stress fields will decrease the discharge capacity of MC C14 Laves phase drastically.

Acknowledgements

The work in this paper is supported by National Advanced Materials Committee and National Natural Science Foundation of China (No. 59601006, 59671016).

References

[1] J. Hout, E. Akiba, T. Ogura, Y. Ishido, J. Alloys Comp. 218 (1995) 101.
[2] A. Züttel, F. Meli, L. Schlapbach, J. Alloys Comp. 231 (1995) 645.
[3] H. Nakano, S. Wakao, J. Alloys Comp. 231 (1995) 587.
[4] J.Y. Yu, Y.Q. Lei, C.P. Chen, J. Wu, Q.D. Wang, J. Alloys Comp. 231 (1995) 578.
[5] S.R. Ovingsky, J.A. Fetcenco, J. Ross, Science 260 (1993) 176.
[6] H. Sawa, S. Wakao, Mater. Trans. JIM 31 (1990) 487.
[7] D. Yan, G. Sandrock, S. Suda, J. Alloys Comp. 316 (1994) 237.
[8] A. Züttel, F. Meli, L. Schlapbach, J. Alloys Comp. 209 (1994) 99.
[9] B.-H. Liu, J.-H. Jung, H.-H. Lee, K.-Y. Lee, J.-Y. Lee, J. Alloys Comp. 245 (1996) 132.
[10] J. Chen, D.H. Bradburst, S.X. Duo, H.K. Liu, J. Alloys Comp. 265 (1998) 281.
[11] M. Ciureanu, J.O. Ström-Olsen, D.H. Ryan, P. Rudkowska, B. Bondoc, J. Electrochem. Soc. 141 (1994) 3291.
[12] S. Fujiwara, B. Kurishinann, Y. Moriwaki, I. Matsumoto, Electrochem. Soc. Proc. 94–27 (1994) 172.
[13] K.Y. Shu, Y.Q. Lei, X.G. Yang, G.F. Lin, Q.D. Wang, G.L. Lü, L.S. Chen, J. Alloys Comp. 293–295 (1999) 756.
[14] K.Y. Shu, Y.Q. Lei, X.G. Yang, S.K. Zhang, L.S. Chen, G.L. Lu, Q.D. Wang, J. Alloys Comp. 290 (1999) 124.
[15] H. Jones, Rep. Prog. Phys. 36 (1973) 1425.
[16] L. Lutterotti, R. Scardi, J. Appl. Cryst. 251 (1991) 459.
[17] G.L. Lü, K.Y. Shu, L.S. Chen, X.Y. Song, X.G. Yang, Y.Q. Lei, Q.D. Wang, J. Alloys Comp. 293–295 (1999) 107.
[18] K.Y. Shu, X.G. Yang, S.K. Zhang, G.L. Lü, Y.Q. Lei, Q.D. Wang, J. Alloys Comp. 306 (2000) 122.